

FLUORESCENT ULTRAMICROSCOPY

PACS numbers: 87.64.M–; 42.81.Wg; 33.50.–j
DOI: 10.1070/QE2010v040n09ABEH014344

Fibreoptic fluorescent microscopy in studying biological objects

A.N. Morozov, A.A. Lazutkin, I.V.Turchin, V.A. Kamenskii, I.I. Fiks, D.V. Bezryadnov, A.A. Ivanova, D.M. Toptunov, K.V. Anokhin

Abstract. **The method of fluorescent microscopy is developed based on employment of a single-mode fibreoptic channel to provide high spatial resolution 3D images of large cleared biological specimens using the 488-nm excitation laser line. The transverse and axial resolution of the setup is 5 and 13 μm, respectively. The transversal sample size under investigation is up to 10 mm. The in-depth scanning range depends on the sample transparency and reaches 4 mm in the experiment. The 3D images of whole mouse organs (heart, lungs, brain) and mouse embryos obtained using autofluorescence or fluorescence of exogenous markers demonstrate a high contrast and cellular-level resolution.**

Keywords: *optical microscopy, light-sheet fluorescence microscopy, 3D-visualisation, brain, biopsy.*

1. Introduction

Optical methods used to obtain 3D images of biological objects with the spatial resolution of about 5 μm needed for viewing separate cells are in demand in modern neurobiology, developmental biology, and experimental medicine. Presently, the most popular method for such investigations is the confocal laser scanning microscopy (CLSM) [1]. It is used to obtain 3D images of biological tissues with a sub-cell resolution to the depth of up to 200–300 μm with the single-shot viewing domain from 0.1 to 0.5 mm [2]. However, understanding the structural and functional organisation for many biological objects, organs, and tissues requires viewing their cell structure in scales comparable to the dimensions of the objects and organs.

Optical methods capable of such viewing large optically transparent samples to a considerable depth with a sub-cell resolution have begun to appear in recent years. These methods are developed in two main directions: optical projection tomography (OPT) [3] and light-sheet fluorescence microscopy (LSFM) [4]. Presently, LSFM is the most promising from the two directions and is actively developed in the following several modifications: selective plane illumination microscopy [5], ultramicroscopy [6], objective coupled planar illumination microscopy [7], and other [4]. The principal distinction between LSFM and CLSM is that the fluorescence is excited only in a narrow layer of a biological tissue due to special illumination systems and the fluorescence is detected in the direction normal to the illumination plane. This prevents the direct laser radiation from passing to the detection channel of the system and eliminates parasitic background light beyond the investigation domain. Such methods provide high resolution at long depths in optically transparent samples even if objectives with a moderate numerical aperture and large flange focal distance are used [6].

In the setups described in literature, the illuminating beams are formed by open systems. This imposes certain constraints on their applications [6]. The present work is aimed at developing the method of fibreoptic fluorescence microscopy [6]. For this purpose we created a compact system for transporting a laser radiation from a source to the object on the basis of a single-mode fibreoptic channel. High resolution of the system is provided by forming a narrow laser illumination beam with the width corresponding to a transverse dimension of the object under study. The beam width was at least 10–20 mm at the thickness from 6 to 25 μm.

Main advantages of such solution as compared to open systems are as follows: high quality of the illumination beam in the investigation domain due to a Gaussian shape of a spatial mode, system insensitivity to external factors (temperature, vibrations, and dust), simplicity of employment and movement. On this basis, the experimental setup for fibreoptic fluorescence microscopy was created and tested on whole clarified samples of the biological tissue.

2. Experimental setup

The experimental setup for fibreoptic fluorescence microscopy is schematically shown in Fig. 1. Fluorescence in preliminarily prepared samples was excited by a 500-mW, 488-nm Coherent Sapphire 488 HP laser (USA), which included the system for radiation delivery into a single-mode optical fiber. A fibreoptic power splitter directs the laser radiation into two illumination arms in the ratio 1:1. Employment of a double-sided illumination scheme provided almost twice the effective investigation area in the x direction of the sample (see Fig. 2). A collimated beam widened to 30 mm in diameter passed through a rectangular (20×4 mm) aperture diaphragm and was focused by a cylindrical lens to the sample placed inside a glass cell filled with immersion liquid (Murray clarifier [8]).

The illumination beam after the orifice becomes almost uniform in the y direction and has the width of 20 mm. In the longitudinal direction x according to [9] the thickness of the Gaussian beam is given by the formula

A.N. Morozov, I.V.Turchin, V.A. Kamenskii, I.I. Fiks Institute of Applied Physics, Russian Academy of Sciences, ul. Ul'yanova 46, 603950 Nizhnii Novgorod, Russia; e-mail: morozov@ufp.sci-nnov.ru;
A.A. Lazutkin, D.V. Bezryadnov, A.A. Ivanova, D.M. Toptunov, K.V. Anokhin P.K. Anokhin Scientific Research Institute of Normal Physiology, Russian Academy of Medical Sciences, ul. Mokhovaya 11, 125009 Moscow, Russia; e-mail: k.anokhin@gmail.com

Received 19 April 2010; revision received 8 July 2010
Kvantovaya Elektronika **40** (9) 842–846 (2010)
Translated by N.A. Raspopov

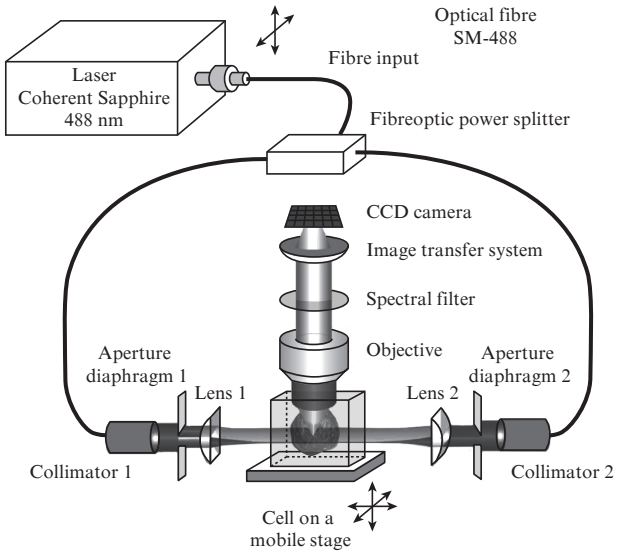

Figure 1. Schematic of the setup for fibreoptic fluorescence microscopy.

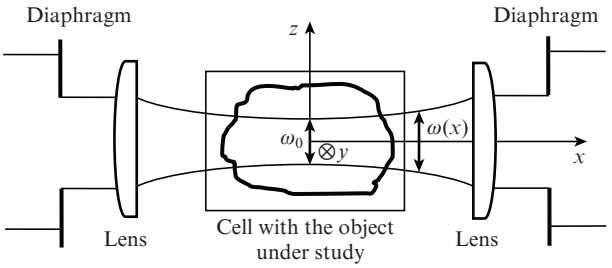

Figure 2. Schematic of the illumination unit for the fluorescence microscopy setup.

$$\omega^2(x) = \omega_0^2\left[1 + \left(\frac{2\lambda x}{\pi\omega_0}\right)^2\right],$$

where λ is the laser radiation wavelength; ω_0 is the beam minimal thickness. The length of the Rayleigh waist is $x_R = \pi\omega_0^2/4\lambda$.

Knowing the cell dimensions, one can calculate variation in the illumination domain thickness in the sample plane for determining the illumination inhomogeneity. To cover a wide range of dimensions for objects under investigation (from several millimeters to several centimeters) with an optimal resolution, we used in the experiments a set of three cylindrical Thorlabs lenses with the focal lengths $F = 40$, 80, and 150 mm. The corresponding beam thicknesses are presented in Table 1.

The radiation excited in the sample was analysed by an Olympus MVX10 fluorescence microscope (Japan) with a planapochromatic objective (M = 1×, WD = 65 mm, NA = 0.25), selected by the narrow-band spectral Chroma Technology filter (λ = 505–530 nm), and detected by a 3.2-megapixel (2184×1472) cooled CCD Alta U32 camera (Apogee Inc., USA). A vertical movement of the sample relative to the plane laser beam was synchronised with the shift of microscope focus by means of step motors controlled by the Objective Imaging software (Great Britain). For each new position of the sample the microscope focusing system was automatically adjusted.

Samples were investigated in 40×20×20-mm quartz cells with the cell wall thickness of 2 mm. Samples clarified by the protocol [8] were glued by a small drop of cyanoacrylate adhesive to a microglass and placed to the cell bottom. The cell was filled with a clarifying solution in such a way that the upper solution level covered the upper boundary of the sample. Scanning was performed at the laser power needed for signal imaging with a sufficient signal-to-noise ratio, which was not above 50% of the total power. An array of two-dimension images (optical cuts) of fluorescing sample was formed during synchronised automated vertical movements of the microscope stage with the sample, which were stepwise photographed. The time needed for obtaining the array of 300 images with resolution of 2184×1472 took about 10 min. The object 3D images were then mathematically processed and rendered by means of the commercial Amira 4 software (Mercury Computer Systems, USA).

3. Estimate of the spatial resolution for the method

The spatial resolution of the method was estimated by a specially made model medium that included fluorescence microparticles of spherical shape with the diameter of 4 μm having the central excitation/absorption wavelengths of 505/515 nm, respectively (FluoSpheres®, Invitrogen, USA). The microspheres were placed into 1% agarose gel having a low-temperature melting point (Sigma, USA) with the subsequent creation of cubes 5 mm^3 in volume. The created model objects placed into distilled water were scanned with the ultramicroscope (the scanning depth step was 1 μm) using a planapochromatic objective (M = 1×, NA = 0.25), magnification 6.3×, and a lens unit for laser illumination with the focal length of 40 mm. The single pixel dimension of the CCD camera on the obtained images was 1.7 μm.

Packets of 2D images obtained during scanning were used for determining the dimensions of fluorescing domains. Figure 3 shows the intensity profile cross sections for the fluorescence of a calibrated microsphere in three planes and their approximation by the Lorentz curve, because it is known that the point blurring function is close to the Lorentz function. If two point objects are separated by a distance longer than the Lorentz curve width calculated for the 0.77 level then they can be separately detected. Therefore, we take this width as the resolution of the fluorescence microscopy method. The calculated average optical resolution and its standard deviation (SD), calculated over an ensemble of realisations are given in Table 2.

Table 1. The minimal thickness of illuminating beam ω_0 and the length of Rayleigh waist x_R employing lenses with different focal length F.

F/mm	ω_0/μm	x_R/μm
40	6	62
80	12	251
150	23	873

Table 2. The transversal and longitudinal optical resolution for the method of fluorescence microscopy.

	z	y	x
Average/μm	13	7	5
RMS/μm	6	3	1

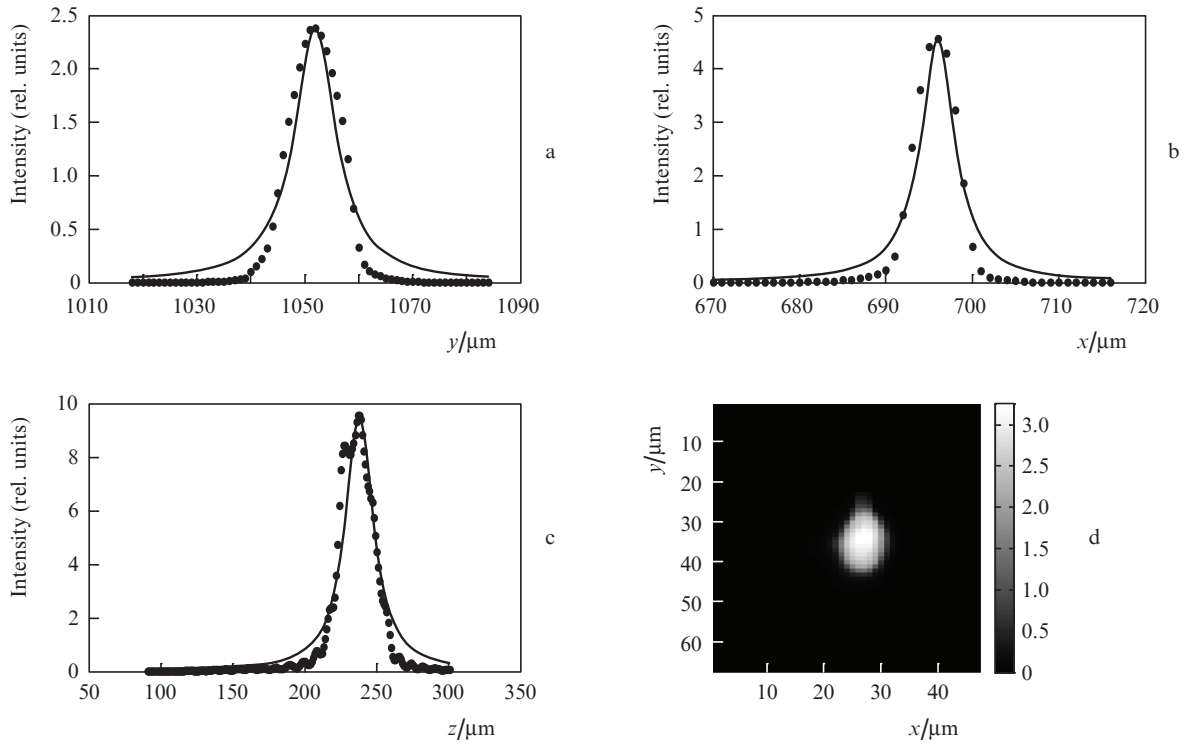

Figure 3. Cross section of the fluorescence intensity profile for calibrated microsphere with the diameter of 4 μm approximated by the Lorentz curve (solid curve) along the *y* axis (a), *x* axis (b), *z* axis (c), and in the *xy* plane (d).

4. Results of 3D rendering

Optical cuts and 3D images of preliminarily clarified samples of biological tissues (whole lungs, heart and brain of mouse embryos and embryos) were obtained by employing specific staining of tissues and autofluorescence emission.

The samples of two-week mice were stained for Egrl protein by using specific antibodies and Alexa488 fluorophore (Invitrogen, USA). Egrl protein expression in brain initiated by nervous activity represents plastic rearrangements in neurocytes and is used for mapping the domains and brain cells that participate in training, memory, and response to stress [10, 11]. Stained preparations subjected to optical clarification by the Murray composition [8] became optically totally transparent, which made it possible to scan them over the whole thickness (3.0 mm). On the brain optical microscopic sections obtained with the laser illumination lenses having a focal length of 80 mm, separate neuron nuclei comprising Egrl protein became distinguished starting with the magnification $2.5^{\times}$. The field of the camera view at such magnification was 6 mm along the large side. This provided viewing optical sections of newborn mice brain as a whole. Thus, the maximal dimensions of the investigated brain samples of a newborn mouse were 5.5×4.7×3.0 mm. An example optical section and 3D image reconstructed from the 200 optical sections made with a step of 15 μm and magnification of $2.5^{\times}$ are presented in Fig. 4.

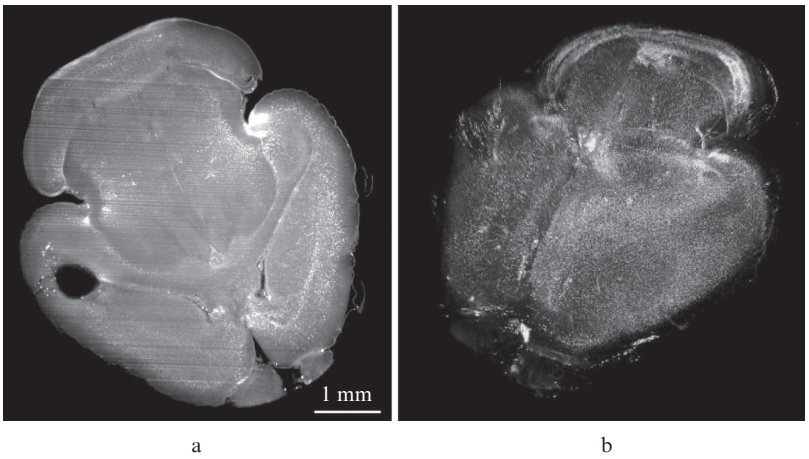

Figure 4. View of Egrl protein in the whole brain of a two-day mouse: the optical section at the depth of 1.5 mm (a) and 3D reconstruction (b).

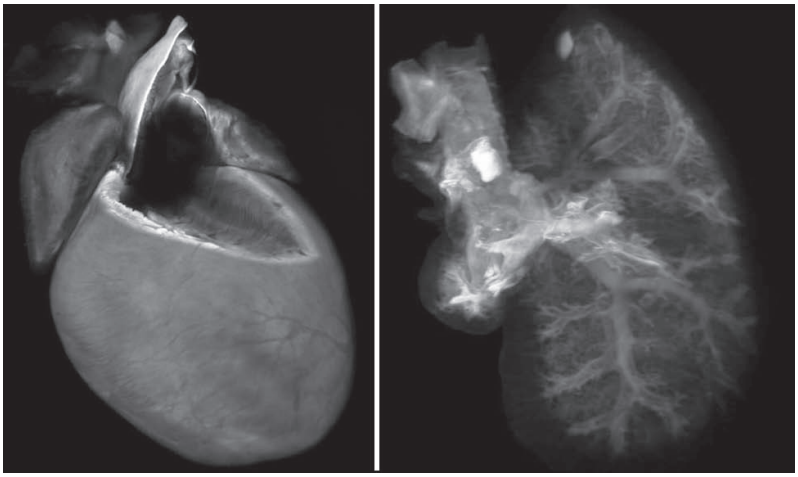

a b

Figure 5. 3D reconstruction of a heart structure with a cross section in the upper part of left ventricle (a) and lung lobe (b) of mouse, obtained by means of autofluorescence.

Figure 5 presents the results of 3D viewing based on autofluorescence of biological tissues. Quite a number of molecules comprised in organism tissues (oxidised flavine forms, porphyrins, aromatic amino acids, pyridoxine, melanin, some structural proteins – collagen, elastin) are endogen fluorophores [12]. It was shown that organs and tissues with a high content of these molecules (blood vessels, spleen, and lymph nodes) exhibit especially high autofluorescence [12]. Our observations and data of other authors [12, 13] prove the possibility of employing autofluorescence for obtaining additional valuable information on the object under study, in particular, for determining morpho-anatomic and histological boundaries and specificities of organs and tissues without using staining agents. In the present work, autofluorescence of entire organs and mice embryos is studied by means of the experimental setup for fibreoptic microscopy.

The samples of entire organs (mouse heart and lungs) were scanned by using laser illumination lenses with the focal length of 80 mm. The scanning was performed over the whole depth of organs. The dimensions of viewed objects after optical clarification were $11\times5\times4$ mm for the mouse heart and $10\times8\times3$ mm for lung. On optical sections obtained in the scanning one clearly distinguishes a histological structure of organs. The morphological features distinct on the optical sections are also distinct on 3D reconstructions: muscle fibers and vascularity are well viewed in the heart (Fig. 5a); in lungs, bronchial tube structures and bronchiole branching are observed (Fig. 5b). Absence of cell structures on the images is explained by the fact that endogen fluorophores are not strongly localised inside cells of organs under investigation.

Example 3D reconstructions of a 14-day mouse embryo are shown in Fig. 6. The sample dimensions are $5.5\times8\times3$ mm.

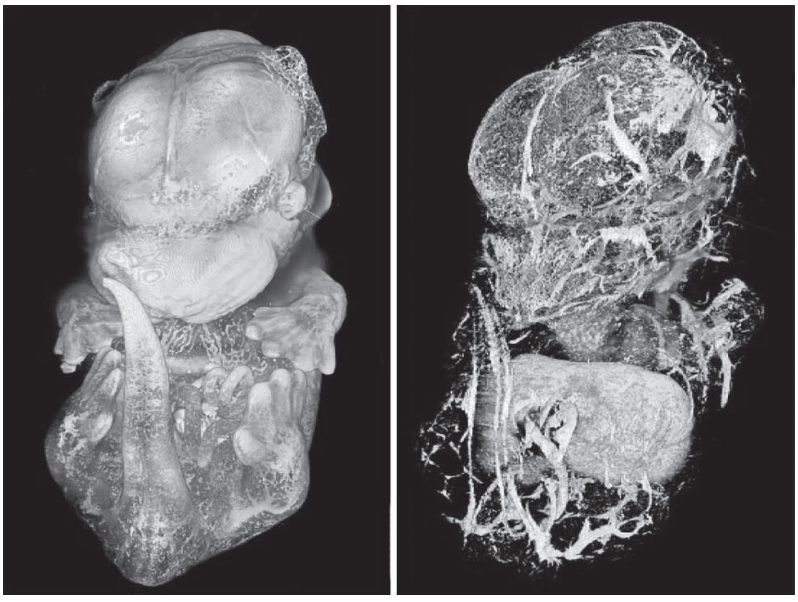

a b

Figure 6. 3D reconstruction of the structure of the 14-day mouse embryo: reconstruction of the surface (a) and internal structure (b).

The reconstructions obtained allow 3D viewing of the embryo body surface and reveal the distinct features of developmental stages such as the degree of evolution for vibrissae, limb fingers, and internal structure (vessels, heart, liver, and other internal organs). At large magnification one can also thoroughly study the vascular system of vibrissae, limbs, and other organs.

Thus, by the examples of clarified samples of biological objects, tissues, and other organs, principal possibilities of the developed experimental setup for fibreoptic fluorescence microscopy are demonstrated. The method makes it possible to view gene expression at cell resolution on microscopic slides having the dimensions of up to 6 mm to the depth of up to 3 mm, as well as fine morphological features of the structure of embryo and internal organs with the dimensions of up to 11 mm to the depth of up to 4 mm. 3D images obtained by means of fluorescence microscopy may be used in medical-biological investigations of an action of new medicines on molecular processes in organism tissues, in working with experimental disease models (for example, cerebral ischemia, heart ischemia, and so on) and biopsy samples in medical diagnosis, as well as for mapping gene expression in whole samples of biological tissues.

5. Conclusions

The setup is developed for fluorescence microscopy on the basis of double-sided single-mode fibreoptic tract for exciting fluorescence at the wavelength of 488 nm. Optical sections and 3D images are obtained for preliminarily clarified samples of biological tissues (lungs, heart, perinatal mouse brain, and mouse embryos) by using immune histochemical staining and autofluorescence. The high resolution of the method is demonstrated (5–13 μm) for large dimensions of objects under investigation (up to 10 mm). The depth of scanning depends on the sample transparency and reaches 4 mm. These parameters noticeably surpass those obtained in the traditional confocal microscopy. The results obtained are quite important in thorough investigations of structural and functional features of structure of organs and tissues in evolution biology, neurobiology, and experimental medicine.

Acknowledgements. The authors are grateful to E.A. Sergeeva and N.M. Shakhova for fruitful discussions in writing the article. The work was supported by the Russian Foundation for Basic Research (Grant No. 06-04-08353-ofi) and Ministry of Education and Science of Russian Federation (State Contract No. 02.522.11.2002).

References

1. Powley J.B., *Handbook of Biological Confocal Microscopy* (New York: Plenum, 1995).
2. Gladkova N.D. *Opticheskaya kogerentnaya tomografiya v ryadu metodov meditsinskoi vizualizatsii* (Optical Coherent Tomography in Series of Medical Viewing Methods: Lecture curses) (N. Novgorod: Institute of Applied Physics, Russian Academy of Sciences, 2005).
3. Sharpe J., Ahlgren U., Perry P., Hill B., Ross A., Hecksher-Sorensen J., Baldock R., Davidson D. *Science*, **296**, 541 (2002).
4. Huisken J., Stainier D.Y. *Development*, **136** (12), 1963 (2009).
5. Huisken J., Swoger J., Del Bene F., Wittbrodt J., Stelzer E.H. *Science*, **305**, 1007 (2004).
6. Dodt H.U., Leischner U., Schierloh A., Jährling N., Mauch C.P., Deininger K., Deussing J.M., Eder M., Zieglgänsberger W., Becker K. *Nature Meth.*, **4**, 331 (2007).
7. Holekamp T.F., Turaga D., Holy T.E. *Neuron*, **57**, 661 (2008).
8. Dent J.A., Polson A.G., Klymkowsky M.W. *Development*, **105**, 61 (1989).
9. Born M., Wolf E. *Principles of Optics* (London: Pergamon, 1970; Moscow: Nauka, 1973).
10. Guzowski J.F., Timlin J.A., Roysam B., McNaughton B.L., Worley P.F., Barnes C.A. *Curr. Opin. Neurobiol.*, **15**, 599 (2005).
11. Knapska E., Kaczmarek L. *Prog. Neurobiol.*, **74**, 183 (2004).
12. Deeb S., Nasr K.H., Madhy E., Badawey M., Badey M. *Afr. J. Biotechnol.*, **7**, 504 (2008).
13. Monici M. *Biotechn. Ann. Rev.*, **11**, 227 (2005).